JOURNAL OF WATER AND LAND DEVELOPMENT
e-ISSN 2083-4535

Polish Academy of Sciences (PAN) Institute of Technology and Life Sciences – National Research Institute (ITP – PIB)

JOURNAL OF WATER AND LAND DEVELOPMENT
DOI: 10.24425/jwld.2026.158713
2026, No. 69 (IV–VI): 157–168

Using quality indices to evaluate groundwater quality in the semi-arid Guorriguer Plain, Tebessa, northeastern Algeria

Djemoui Mamour*[1)], Samia Halimi[1)], Nadhir Bouchema[2)], Hichem Khammar[2)], Karima Boukhallat[1)]

[1)] Laboratory of Biotechnology, Water, Environment and Health, Department of Ecology and Environment, Faculty of Natural and Life Sciences, University of Abbes Laghrour, Khenchela, P.O. Box Khenchela 40000, Algeria

[2)] Laboratory of Functional Ecology and Environment, Department of Life Sciences and Nature, Faculty of Exact and Life Sciences, University of Larbi Ben M'hidi, P.O. Box 04000, Oum El Bouaghi, Algeria

* Corresponding author

RECEIVED 01.09.2025 ACCEPTED 07.01.2026 AVAILABLE ONLINE 16.06.2026

Abstract: To assess groundwater quality in the semi-arid Guorriguer Plain, Tebessa, northeastern Algeria, two indices were used: the water quality index (*WQI*) and the groundwater pollution index (*GPI*). Accordingly, the physical and chemical parameters of 21 groundwater wells were evaluated. Field measurements included pH, temperature, and electrical conductivity, while cation and anion concentrations were analysed in the laboratory. The results show that groundwater resources in the study area are mostly suitable for drinking. A comprehensive assessment of water quality using the *WQI* and *GPI* standard indices revealed that approximately 90% of the sampled wells met permissible quality thresholds, with many classified as "excellent" to "good" (*WQI* < 200). This was confirmed by parallel *GPI* assessments, which indicated that 90% of samples showed only "minor pollution" to "slight pollution" (*GPI* < 1.5), suggesting minimal human impact in most areas. However, clear localised deterioration was observed in 10% of the samples located along the southwest-to-northeast axis, where high total dissolved solids (TDS) values (1500–3189 mg·dm^{-3}) and specific conductivity (>2000 μS·cm^{-1}) exceeded recommended limits. This was primarily due to the influence of geological formations and, secondarily, to agricultural activity characteristic of this region. This study contributes to a deeper understanding of groundwater quality dynamics in semi-arid regions by integrating several indicators and examining their relationships with natural and human factors to obtain accurate results that can help the responsible authorities improve the management and conservation of these important resources.

Keywords: groundwater, groundwater pollution index (*GPI*), Guorriguer Plain, pollution, water quality index (*WQI*)

INTRODUCTION

Groundwater is a critical freshwater resource, particularly in semi-arid regions where surface water availability is limited due to low rainfall, high evaporation rates, and prolonged droughts (Jia *et al.*, 2020). In such water-stressed environments, groundwater serves as the primary source for drinking, irrigation, and industrial needs, making its quality a crucial factor in socio-economic stability and ecosystem health (Adimalla and Taloor, 2020). However, growing anthropogenic pressures, including agricultural intensification, untreated wastewater discharge, and overexploitation, coupled with climate-induced aridity, are exacerbating groundwater pollution and depletion, threatening long-term water security (Li, He and Guo, 2019; Li, Wu and Qian, 2022).

The Guorriguer Plain, located in a semi-arid zone, exemplifies these challenges. Characterised by scarce and erratic rainfall, high temperatures, and elevated evapotranspiration rates, the region relies almost exclusively on groundwater to meet its water demands (Barakat *et al.*, 2021). However, the combination of low recharge rates and increased consumption, together with increasing pollution from fertilisers, waste, and sewage, has raised concerns about the sustainability of this vital resource (Mukate *et al*., 2019). In such hydroclimatic conditions, pollutants become more concentrated because of limited dilution, further degrading water quality and posing health risks to dependent communities (Karunanidhi *et al*., 2021).

Traditional water quality assessments, which rely on comparing individual parameters with regulatory standards, often fail to capture the cumulative impact of multiple contaminants or the influence of climatic stressors (Boateng *et al*., 2020). To overcome this limitation, composite indices such as the water quality index (*WQI*) and groundwater pollution index (*GPI*) provide a robust framework for assessing overall water suitability by integrating physicochemical and geochemical data into interpretable scores (Bahrami Asl *et al.* (2025). The *WQI* is particularly useful for classifying water into categories (e.g., excellent to unsuitable) based on its suitability for human consumption (Horton, 1965), while the *GPI* helps identify pollution sources and assess contamination risks, especially in regions vulnerable to anthropogenic and climatic pressures (Zahedi, 2017).

In this study, we adopted the *WQI* and *GPI* to assess groundwater quality. While both indices rely on physicochemical parameters, their combined application provides a more nuanced evaluation by distinguishing between general potability and potential contamination risks. Our approach emphasises spatial heterogeneity in groundwater quality in relation to geological and hydrogeological structures. This methodological integration represents a significant contribution, as it demonstrates how multiple indices can complement one another to provide a more robust tool for groundwater quality assessment in semi-arid regions.

The findings will provide critical insights for policymakers to implement adaptive water management strategies, such as regulated extraction, pollution control measures, and artificial recharge techniques, to enhance groundwater resilience in water-scarce regions.

MATERIALS AND METHODS

STUDY AREA

In northeastern Algeria, the Guorriguer Plain extends from the province of Tebessa to the provinces of Khenchela and Oum El Bouaghi and lies between 35°58'82" and 35°32'58" N latitude and 7°74'85" and 7°45'88" E longitude. The plain covers approximately 658 km^2 and has an average altitude of 1,000 m a.s.l. (Fig. 1). The study area has a semi-arid climate, with an average annual temperature of 15.4°C and approximately 386.9 mm of rainfall annually.

GEOLOGICAL AND HYDROGEOLOGICAL FRAMEWORK OF THE STUDY AREA

The study area features a complex stratigraphic succession spanning Triassic to Quaternary deposits, reflecting its dynamic geological and tectonic history. The Triassic sequence is characterised by evaporite formations that have undergone significant halokinetic processes, contributing to regional subsidence patterns. Cretaceous units (Cenomanian to Campanian) display considerable lithological diversity, with prominent exposures of Maastrichtian limestone formations at Djebel

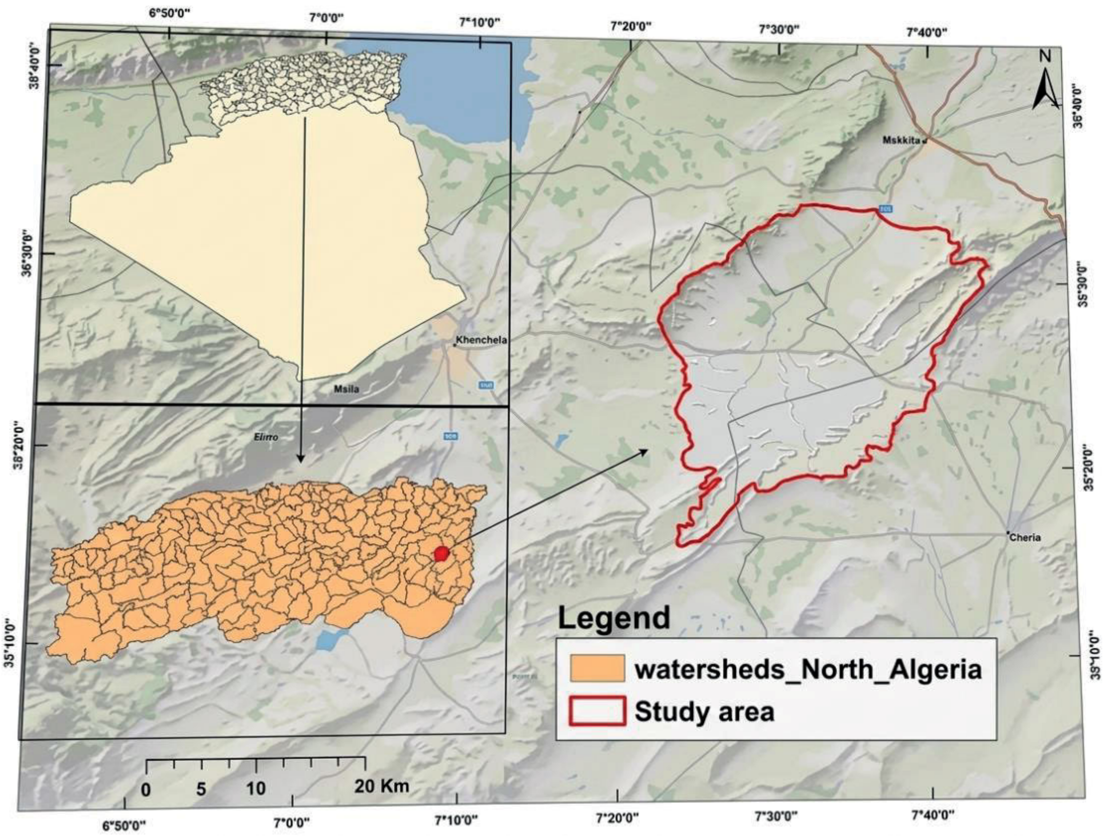

Fig. 1. Location map of the study area, the Guorriguer Plain; source: own elaboration

Guorriguer. The Paleogene–Neogene succession consists mainly of marls and biomicrites, especially in Paleocene and Eocene strata. The most recent Mio-Plio-Quaternary aquifer system comprises alternating sandstone, conglomerate, and clay deposits, indicative of active sedimentary processes (Djelel, 2014; Hireche, 2014) – Figure 2. This comprehensive stratigraphic framework provides critical context for understanding the region's hydrogeological characteristics and groundwater dynamics. The main freshwater resources are hosted in the Quaternary aquifer. This aquifer consists of unconsolidated alluvial deposits (gravels, sands, and silts) with medium to high permeability, making it the most productive and exploited groundwater body.

Piezometric measurements recorded at the sampling points in June 2023 enabled us to create a piezometric map (Fig. 2). Interpretation of this map showed that:

– the general flow direction is from southwest to northeast,
– the aquifer in the study area receives water from the highlands surrounding the area on the southern and southwestern sides.

The hydraulic gradient is weak in the northeastern areas and strong in the southwestern area. This variation in gradient results, on the one hand, from the significant slope in the southern and southwestern parts and, on the other hand, from pumping activity in the low-lying area. Recharge mainly occurs through direct rainfall infiltration, indirect infiltration from ephemeral wadis during floods, and irrigation return flow. The Quaternary aquifer is hydraulically connected to surface water systems, switching between recharge and discharge zones depending on seasonal conditions. Due to its shallow depth and direct surface interaction, this aquifer remains highly vulnerable to contamination from agricultural activities and wastewater from domestic sources.

SAMPLING AND LABORATORY ANALYSIS

The assessment of water resource quality in the study area involved analysing multiple datasets, with a particular focus on groundwater, which is widely used for drinking and agricultural purposes. In this study, groundwater quality was evaluated using 16 physicochemical parameters measured in 21 samples collected at different locations in July 2023 (Fig. 3). Groundwater samples were collected following international standards recommended by the World Health Organization (WHO, 2011) and the American

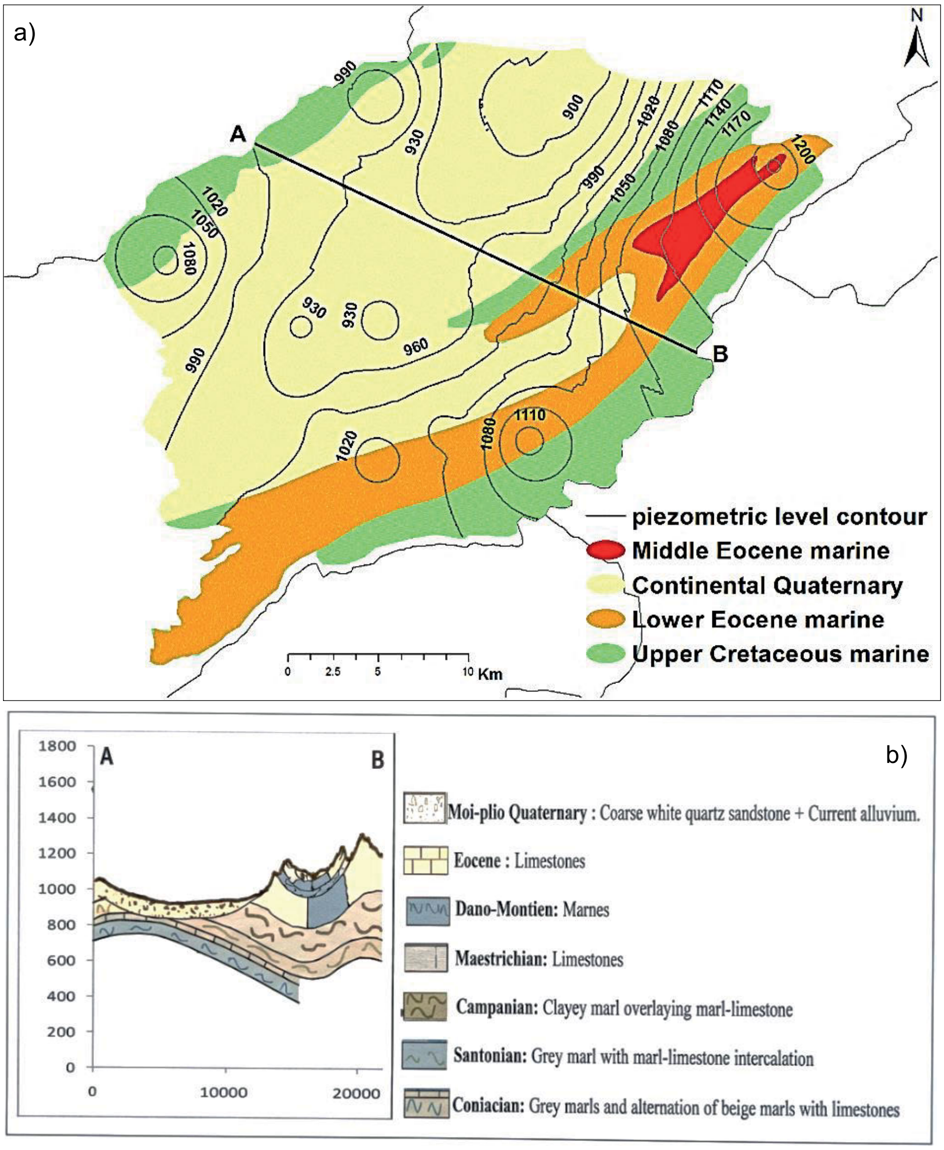

Fig. 2. Guorriguer Plain: a) geological map, b) cross section; source: own elaboration

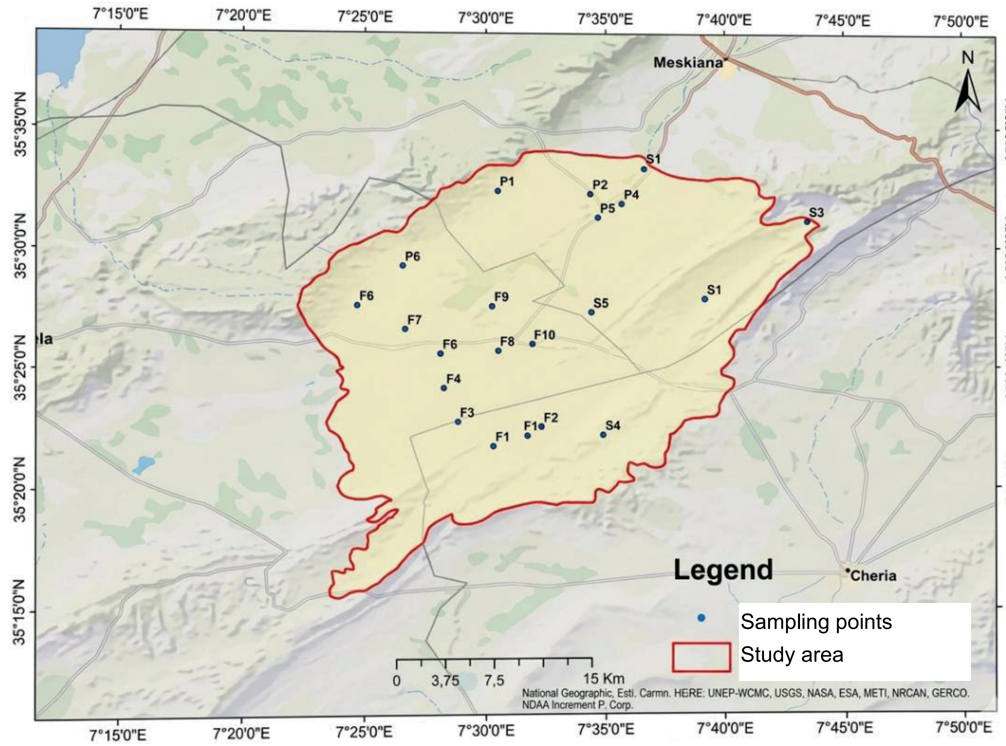

Fig. 3. Sampling points in the study area; the characters F, S, and P were used for sample labelling purposes only; source: own elaboration

Public Health Association (Rice, Baird and Eaton, 2017) to ensure representativeness and reliability. The protocol included pumping and flushing each well before sampling to remove stagnant water and obtain fresh groundwater. According to best practices, wells were pumped continuously for at least 5–10 minutes, or until the physicochemical parameters, including pH, electrical conductivity (*EC*), dissolved oxygen (DO), total dissolved solids (TDS), and temperature, stabilised before sample collection. This step is essential to avoid artefacts caused by mixing with stored water in the well casing. In practice, the pumping time was recorded for each well, and water quality stabilisation was verified in situ with a DSS-16K102315 digital multiparameter probe. Once equilibrium was achieved, samples were collected in pre-cleaned polyethylene bottles, preserved according to the parameter analysed (acidification for cations and refrigeration for nutrients), and transported under cold conditions to the laboratory. This approach ensured that the analysed samples accurately reflected the aquifer's hydrochemical conditions rather than well-storage effects. In the laboratory, total hardness (*TH*) was measured using the EDTA titrimetric method. Additionally, chemical parameters such as Na^+, K^+, Ca^{2+}, Mg^{2+}, $Cl^−$, $SO_4^{2−}$, $PO_4^{3−}$, $HCO_3^−$, $NO_3^−$, $NO_2^−$, and NH_4^+ were analysed (see Tab. 1). Before measuring major ion concentrations (Na^+, K^+, and Ca^{2+}), the samples were filtered through 0.45 μm cellulose membranes. All chemical analyses were conducted at the Functional Ecology and Environment Laboratory following the methodologies outlined by Rodier (2009).

SPATIAL ANALYSIS

The study relied on spatial variation analysis of the physical and chemical parameters of groundwater, linking them to the geological and hydrogeological characteristics of the area.

Table 1. Analytical techniques and parameters for water quality assessment

Parameter	Technique
Na^+, K^+ and Ca^{2+}	flame emission spectrometry
SO_4^{2-}, NO_3^-, NO_2^-, NH_4^+ and $PO_4^{3−}$	visible UV spectrometry
Mg^{2+}, HCO_3^- and Cl^-	titration

Source: own elaboration.

Geographic Information System (GIS) techniques were employed to map the spatial distribution of the studied variables (such as TDS, *EC*, Na^+, Cl^-, and $SO_4^{2−}$), and inverse distance weighting (IDW) interpolation was applied to generate isoline maps. This method transforms discrete sampling data into continuous spatial distributions, allowing reliable estimation of values at unsampled locations and highlighting the spatial variability of physicochemical parameters. This approach enabled the identification of high-concentration and dilution zones and their correlation with the nature of the aquifer formations, particularly Quaternary deposits, as well as with hydrogeological factors such as flow direction and recharge zones (Taloor, 2022).

HYDRO-GEOCHEMISTRY

To identify the natural and human-made processes that influence the chemical composition of groundwater in the study area, as well as to determine the sources of potential pollutants, whether they originate from interactions between water and rock (natural geochemical processes) or from human activities such as agriculture and wastewater discharge, we used the Piper and Gibbs diagrams, along with a land use map and a groundwater vulnerability map. The Piper diagram helps classify water types and analyse the relationships between the main cations and anions, which aids in distinguishing groundwater facies and understanding their geochemical evolution (Kotowski and Satora, 2016). The Gibbs diagram is used to identify the dominant mechanisms affecting groundwater chemistry, such as evaporation, rock-water interaction, and anthropogenic contamination, thereby providing insights into groundwater development and the extent of human impact (Ahamad *et al.*, 2018; Madhav *et al.*, 2018; Adimalla, 2019).

WATER QUALITY INDEX

The water quality index (*WQI*) was used as a reliable quantitative method for comprehensive water quality assessment (Guenouche *et al.*, 2024; Pachiyappan, Cuddalore Thandapani and Kumarasamy, 2025). This integrative approach considers selected essential physicochemical parameters (pH, *EC*, Ca^{2+}, Mg^{2+}, Na^+, K^+, HCO_3^-, Cl^-, SO_4^{2-}, and NO_3^-) in relation to WHO (2011) drinking water standards. As a sensitive indicator of environmental health, the *WQI* combines complex hydrochemical data into a single numeric value, allowing effective groundwater quality evaluation for potability (Li *et al.*, 2023; Jayasankar *et al.*, 2024).

Weighting and calculation methods

Parameter weights (W_i) were assigned according to their health significance and hydrochemical importance (Barki and Singa, 2014; Moeinzadeh, 2024). Critical parameters (*EC*, Mg^{2+}, Na^+, Cl^-, NO_3^-, and SO_4^{2-}) received the maximum weight (W_i = 5), while HCO_3^- was assigned the minimum weight (W_i = 1) due to its limited health impact (Islam, 2023; Luo *et al.*, 2024). Relative weights (rW_i) were calculated as:

$$rW_i = \frac{W_i}{\sum_i^n W_i} \tag{1}$$

where: n = number of parameters, W_i = weight of each parameter, rW_i = relative weight (Tab. 2).

Table 2. Computed values of relative weight (rW_i)

Parameter	Unit	WHO (2011) standard	W_i	rW_i
EC	$\mu S \cdot cm^{-1}$	1,000	5	0.147058824
pH	–	7	3	0.088235294
Ca^{2+}	$mg \cdot dm^{-3}$	75	2	0.058823529
Mg^{2+}	$mg \cdot dm^{-3}$	50	2	0.058823529
K^+	$mg \cdot dm^{-3}$	10	1	0.029411765
Na^+	$mg \cdot dm^{-3}$	200	5	0.147058824
Cl^-	$mg \cdot dm^{-3}$	250	5	0.147058824
SO_4^{2-}	$mg \cdot dm^{-3}$	250	5	0.147058824
NO_3^-	$mg \cdot dm^{-3}$	50	5	0.147058824
HCO_3^-	$mg \cdot dm^{-3}$	300	1	0.029411765
Sum	–	–	**34**	**1.000000000**

Explanations: W_i = weight of each parameter, *EC* = electrical conductivity.
Source: own study.

Quality scaling and index computation

Each parameter's quality ratio (q_i) was determined by:

$$q_i = \frac{C_i}{S_i} 100 \tag{2}$$

where: C_i = measured concentration of each chemical parameter in each water sample ($mg \cdot dm^{-3}$), S_i = WHO standard.

The sub-index (SL_i) and final water quality index (*WQI*) were computed as:

$$SL_i = rW_i \cdot q_i \tag{3}$$

$$WQI = \sum SL_i \tag{4}$$

All categories suggested for *WQI* are illustrated in Table 3.

Table 3. Categories suggested for water quality index (*WQI*)

Class range of *WQI*	Type of water
<50	excellent
50–100	good
101–200	permissible
201–300	doubtful
>301	unsuitable for drinking

Source: own elaboration based on: Li *et al.* (2023), Guenouche *et al.* (2024), Pachiyappan, Cuddalore Thandapani and Kumarasamy (2025).

GROUNDWATER POLLUTION INDEX

The *GPI* provides a methodological approach to measuring the impact of specific variables on overall groundwater quality and was developed by Subba Rao (2012). It is used to determine the relative influence of each water quality parameter (Sanad, 2024) – Table 4. The methodological process for calculating the *GPI* involves five main steps (Rao, 2018) (Tab. 5).

Rao *et al.* (2018) define the groundwater pollution index (*GPI*) as an integrative assessment tool that evaluates cumulative water quality impacts from multiple chemical parameters, generating a unified quantitative measure of pollution severity (Tab. 6).

RESULTS AND DISCUSSION

PIPER DIAGRAM

The Piper diagram (Piper, 1944) demonstrates that the dominant cationic species are Na^+, Ca^{2+}, and Mg^{2+} (Fig. 4), while the dominant anionic species are Cl^- and SO_4^{2-}. The dominant chemical facies are chloride, calcium-magnesium sulphate, and sodium sulphate, which indicate a halite (NaCl) origin related to the geological formations. According to the Piper diagram, the dissolution of gypsum and anhydrite, which are common in the Quaternary rocks of the study area, is the main cause of the high amounts of calcium (Ca^{2+}) and sulphate (SO_4^{2-}) in groundwater.

Table 4. The WHO standards for groundwater quality parameters and their weight values

Parameter	Unit	WHO (2011) standard	*rW*	*Wp*
TDS	$mg \cdot dm^{-3}$	500	2	0.0370
EC	$\mu S \cdot cm^{-1}$	1000	5	0.0925
DO	$mg \cdot dm^{-3}$	5	5	0.0925
pH	–	7	4	0.0740
Ca^{2+}	$mg \cdot dm^{-3}$	75	3	0.0555
Mg^{2+}	$mg \cdot dm^{-3}$	50	3	0.0555
K^+	$mg \cdot dm^{-3}$	10	3	0.0555
Na^+	$mg \cdot dm^{-3}$	200	4	0.0740
Cl^-	$mg \cdot dm^{-3}$	250	4	0.0740
SO_4^{2-}	$mg \cdot dm^{-3}$	250	4	0.0740
PO_4^{3-}	$mg \cdot dm^{-3}$	5	4	0.0740
NH_4^+	$mg \cdot dm^{-3}$	35	3	0.0555
NO_3^-	$mg \cdot dm^{-3}$	50	5	0.0925
HCO_3^-	$mg \cdot dm^{-3}$	300	2	0.0370
TH	$mg \cdot dm^{-3}$	100	3	0.0555
Sum	–	–	**54**	**1.0000**

Explanations: *rW* = relative weight, *Wp* = weight parameter, TDS = total dissolved solids, *EC* = electrical conductivity, DO = dissolved oxygen, *TH* = total hardness.
Source: own study.

GIBBS DIAGRAM

A plot comparing TDS concentrations with the cation ratio $Na^+/(Na^+ + Ca^{2+})$ and the anion ratio $Cl^-/(Cl^- + HCO_3^-)$ was used to examine the influence of evaporation, rock weathering, and atmospheric inputs (Fig. 5). The fact that most of the studied wells fall under the category of evaporation dominance clearly illustrates how evaporation shapes groundwater chemistry. This suggests that evaporation dominance is the main factor influencing elevated salinity levels. Moreover, the amounts of sodium (Na^+) and chloride (Cl^-) in groundwater are probably linked to agricultural fertilisers and irrigation return flows (Subba Rao, 2005; Verma, Yadav and Singh, 2020).

A statistical overview of groundwater quality parameters, including mean, median, minimum, and maximum values, compared to WHO (2011) guidelines is presented in Table 7.

SPATIAL DISTRIBUTION OF PHYSICOCHEMICAL PARAMETER CONCENTRATIONS

Groundwater chemistry in the study area is primarily controlled by water-rock interaction, with increasing influence from human activities. The dissolution of sedimentary rocks, especially evaporites, significantly raises groundwater salinity, while agricultural return flow adds additional salt loading. The spatial distribution of physicochemical parameters, reflecting this dual influence, is shown in Figure 6.

Table 5. Steps of calculating the groundwater pollution index (*GPI*)

Parameter	Equation	Description
Assignment of relative weights (*rW*)	$rWi = \frac{\text{Wi}}{\sum_i^n wi}$ (1)	*rW* on a scale of 1 to 5, indicating their importance in evaluating water quality
Weight parameter (*Wp*)	$Wp = \frac{Rw}{\sum_{i=n}^n Rw}$ (2)	*Wp* is calculated according to the designated weightings (*rW*) for each parameter
Concentration state (*Sc*)	$Sc = \frac{C}{WQS}$ (3)	*C* is concentration of the parameter in a water sample, *WQS* is drinking water quality standard
Overall chemical quality of water (*Ow*)	$Ow = Wp \cdot Sc$ (4)	*Ow* provides an integrated assessment of water quality based on individual chemical components
Groundwater pollution index (*GPI*)	$GPI = \sum_{\text{i}=n}^{n} Ow$ (5)	*GPI* is determined by totalling the *Ow* values for all assessed parameters in each water sample

Source: own study.

Table 6. The groundwater pollution index (*GPI*) classification values

GPI range	Pollution level
<1.0	negligible pollution
1.01–1.50	slight pollution
1.51–2.0	moderate pollution
2.01–2.50	high pollution
>2.51	very high pollution

Source: own elaboration based on: Subba Rao (2012).

High *EC*, $CaSO_4$, and Na^+ values are concentrated in the northeastern basin, indicating interaction with evaporitic formations such as gypsum ($CaSO_4{\cdot}2H_2O$), anhydrite ($CaSO_4$), and halite (NaCl). Their dissolution enriches groundwater with calcium, sulphate, sodium, and chloride, producing elevated *EC* levels typical of areas with intense water-rock exchange. In contrast, the southwestern zone shows low *EC* and ion concentrations, suggesting a recharge area dominated by less soluble rocks, such as sandstone and limestone (Kotowski and Kachnic, 2016). Groundwater here is relatively young and has undergone limited geochemical evolution. This is confirmed by the hydraulic gradient lines and flow directions shown in Figure 2.

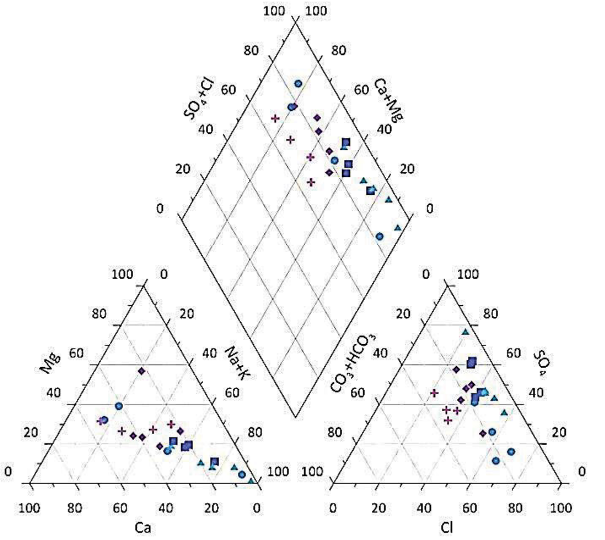

Fig. 4. Piper diagram showing hydrochemical facies of water in Guorriguer Plain; source: own study

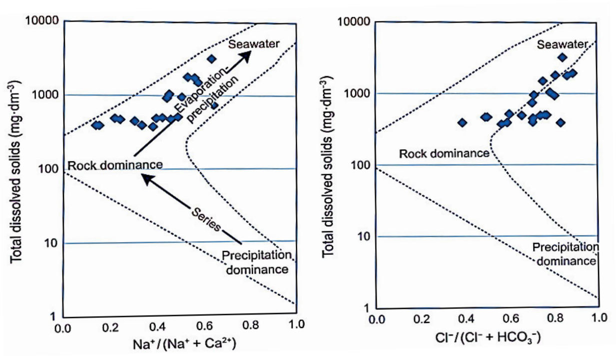

Fig. 5. Gibbs plot showing groundwater geochemical processes in Guorriguer Plain; source: own study

The high Cl^- and SO_4^{2-} levels found in the west and north are likely caused by human activity, including the use of potash fertilisers, irrigation water evaporation, and sewage leaks. Furthermore, where the groundwater is shallow, surface evaporation concentrates salts in the water.

Correlation analysis supports this conclusion: the strong Cl^-–Na^+ relationship (r = 0.893) suggests a common, mainly human-made source such as irrigation return flow, chemical fertilisers, or wastewater infiltration. Likewise, the SO_4^{2-}–Mg^{2+} (r = 0.820) and moderate SO_4^{2-}–Ca^{2+} (r = 0.529) correlations indicate mixed origins, with agricultural inputs being the primary contributor rather than gypsum or anhydrite dissolution.

Overall, the chemical signatures and ion–ion relationships confirm that anthropogenic activities within a semi-arid environment significantly contribute to the salinisation of groundwater in the Guorriguer Plain.

LAND USE IN THE GUORRIGUER BASIN

The 2023 land use map (Fig. 7) shows clear topographic control over spatial patterns in the Guorriguer basin. This distribution reflects both natural factors and human influence, with land use following distinct zones linked to elevation and water availability.

Forested areas in the northern and central highlands are associated with the rain shadow effect. These elevations block residual moist air masses, leading to localised rainfall and creating microclimates that support drought-resistant vegetation.

Along the main valley, there is a linear strip of irrigated farmland where shallow groundwater (about 17–22 m deep) provides a reliable water source, making it the primary factor influencing the distribution of agriculture. However, this farming activity is also considered one source of groundwater pollution due to the use of fertilisers. Extensive bare soils along the wadi

Table 7. Descriptive statistics of the physicochemical parameters in the Guorriguer Plain

Parameter	Unit	Min.	Max.	Average	Median	WHO (2011) standard
T	°C	15.00	25.80	18.44	18.70	25
EC	$\mu S \cdot cm^{-1}$	479.00	4109.00	1223.43	670.00	1,000
TDS	$mg \cdot dm^{-3}$	366	3189	904.71	498	500
DO	$mg \cdot dm^{-3}$	1.70	9.5	7.37	8.16	5
pH	–	7.00	8.65	7.67	7.66	7
Ca^{2+}	$mg \cdot dm^{-3}$	30.00	179.11	65.94	51.30	75
Mg^{2+}	$mg \cdot dm^{-3}$	20.98	191.69	53.92	42.58	30
K^+	$mg \cdot dm^{-3}$	0.11	6.59	1.93	1.72	10
Na^+	$mg \cdot dm^{-3}$	7.63	1,969.52	361.79	101.50	200
Cl^-	$mg \cdot dm^{-3}$	53.25	674.50	223.99	195.25	250
SO_4^{2-}	$mg \cdot dm^{-3}$	60.38	2,171.67	308.53	199.28	250
PO_4^{3-}	$mg \cdot dm^{-3}$	0.05	0.26	0.10	0.09	5
NH_4^+	$mg \cdot dm^{-3}$	0.27	1.07	0.35	0.31	35
NO_2^-	$mg \cdot dm^{-3}$	0.00	0.90	0.06	0.01	3
NO_3^-	$mg \cdot dm^{-3}$	0.08	5.40	2.70	2.50	50
HCO_3^-	$mg \cdot dm^{-3}$	53.68	102.48	72.74	73.20	300
TH	$mg \cdot dm^{-3}$	17.00	114.00	38.95	26.00	100

Explanations: T = temperature, EC = electrical conductivity, TDS = total dissolved solids, DO = dissolved oxygen, pH = potential of hydrogen, TH = total hardness. Source: own study.

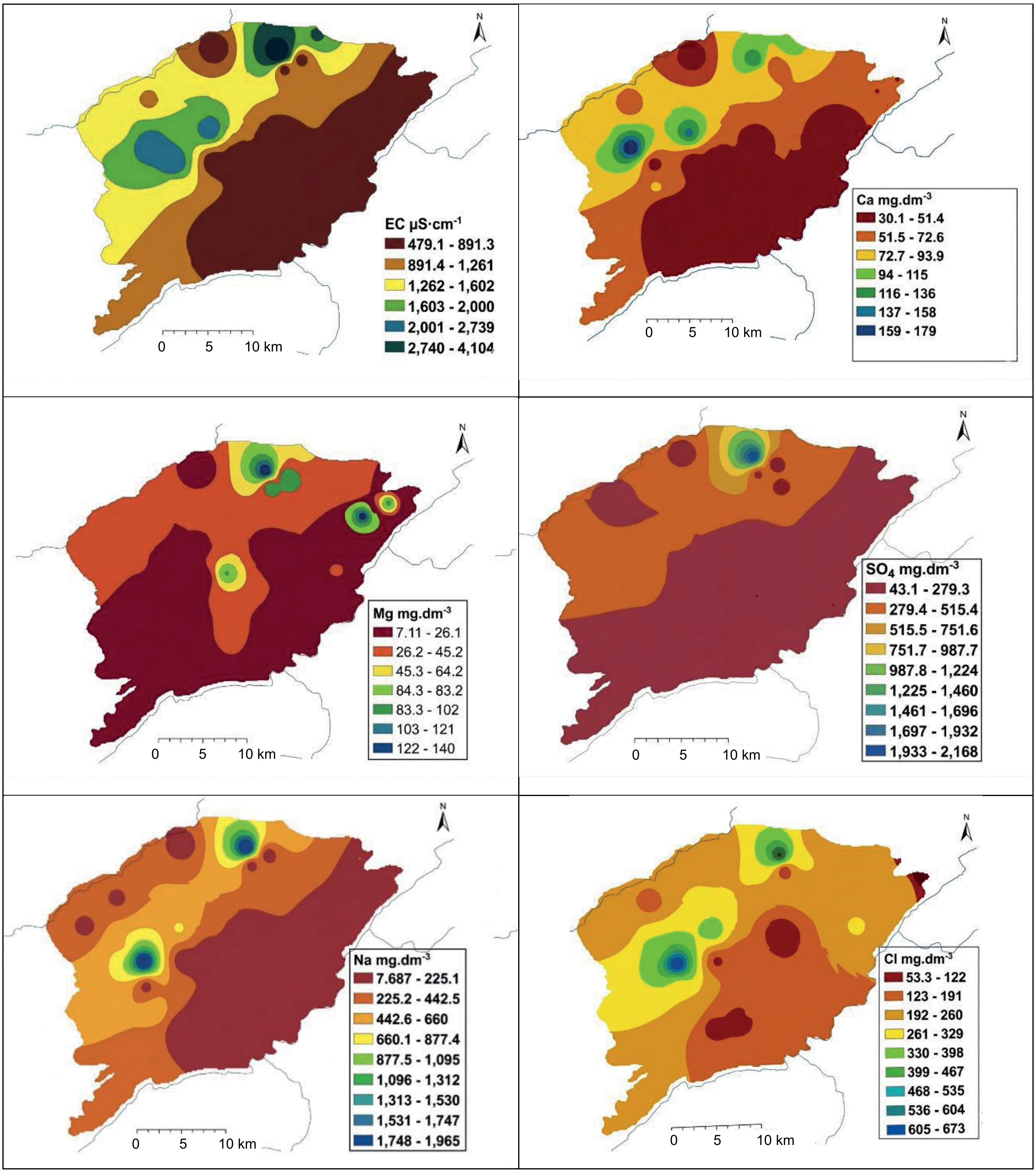

Fig. 6. Spatial distribution maps of physicochemical parameters (*EC* = electrical conductivity, Ca^{2+}, Mg^{2+}, SO_4^{2-}, Na^+ and Cl^-); source: own study

characterise the semi-arid landscape. Low rainfall and high evaporation rates hinder plant growth, reinforcing the dominance of exposed surfaces.

SPATIAL DISTRIBUTION OF GROUNDWATER VULNERABILITY

The map (Fig. 8) shows the DRASTIC (D = depth to water, R = recharge, A = aquifer media, S = soil media, T = topography, I = vadose zone influence, C = hydraulic conductivity) vulnerability index for groundwater in the study area. This index assesses the risk of groundwater pollution by combining various hydrogeological parameters. It reveals a spatial gradient from low to high susceptibility. The highest vulnerability zones are concentrated in the central part of the study area, especially along the main wadi axis. These are surrounded by moderately vulnerable zones and, further out, by low-vulnerability areas mainly located in the northeastern and southwestern sectors. This distribution reflects the influence of key hydrogeological factors controlling contaminant transport.

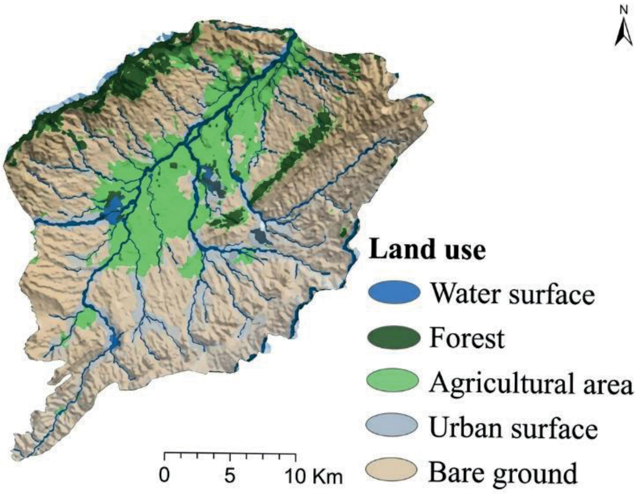

Fig. 7. Land use (2023) map in the Guorriguer Plain; source: own study

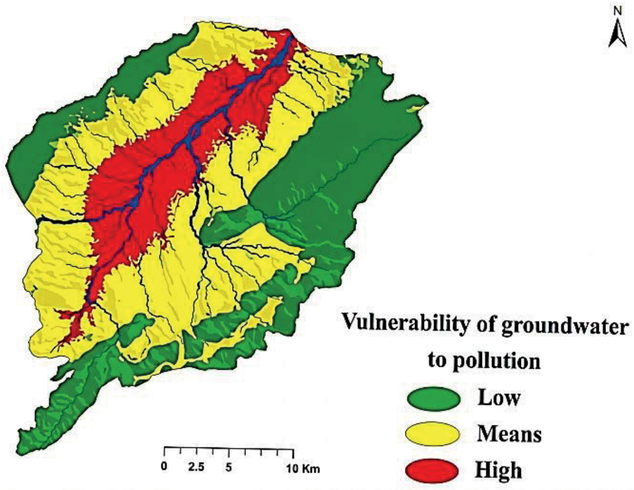

Fig. 8. The DRASTIC vulnerability index (2023) for groundwater in the Guorriguer Plain; source: own study

1. High vulnerability (red zones): these zones occur in regions characterised by highly permeable Quaternary formations composed of unconsolidated sand and gravel, where the groundwater table (approximately 17–22 m deep) is shallow. Such conditions facilitate the rapid infiltration of contaminants with limited filtration capacity. This contributes to part of the groundwater contamination observed in the area, along with the geological nature of the region, which includes evaporitic (saline) rocks.
2. Moderate vulnerability (yellow zones): these zones represent transitional areas consisting of alternating thin layers of clay and sand, with an intermediate groundwater depth and moderate protective capacity.
3. Low vulnerability (green zones): these zones occur in regions with low-permeability rocks acting as protective layers, usually in elevated areas where the groundwater table is deeper (60–90 m), allowing more time for contaminant reduction.

WATER QUALITY INDEX

The calculated water quality index (*WQI*) values (33.664–389.127) showed significant spatial variation in groundwater quality across the Guorriguer Plain (Fig. 9a; Tab. 8). As detailed in Table 3 for water quality categories, approximately 80.95% of samples were classified as excellent to acceptable quality, indicating generally suitable conditions for human consumption. However, the presence of questionable (4.76%) and unsuitable (4.76%) samples highlights localised pollution hotspots, particularly in topographically low-lying areas underlain by Quaternary evaporite deposits (Fig. 2). These spatial patterns reflect the combined influence of geological processes (especially halite and gypsum dissolution), agricultural activities (such as the use of fertilisers and evaporation of irrigation water), and semi-arid climatic conditions (low rainfall and high evaporation and transpiration rates), which increase solute concentration through mineral weathering and evaporative concentration.

GROUNDWATER POLLUTION INDEX

Classifications of water quality based on water quality index (*WQI*) and groundwater pollution index (*GPI*) values are shown in Table 9.

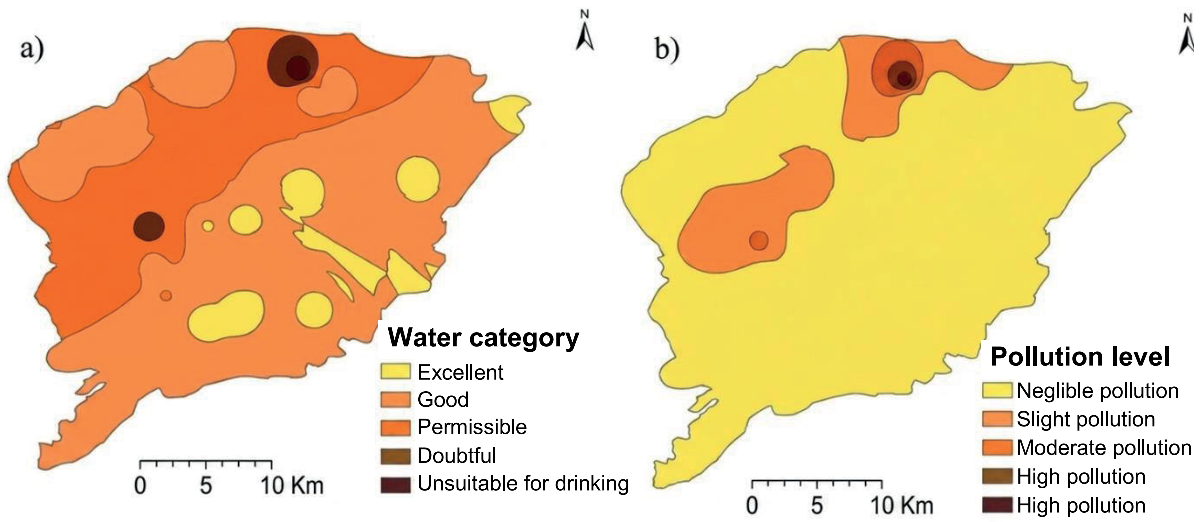

Fig. 9. Spatial distribution of: a) categories of water based on water quality index (*WQI*) values, b) pollution level based on groundwater pollution index (*GPI*) values; source: own study

Table 8. Percentage distribution of samples according to water quality index (*WQI*) classification categories

WQI category	Samples percentage
Excellent (<50)	42.85
Good (50–100)	28.57
Permissible (101–200)	19.04
Doubtful (201–300)	4.76
Unsuitable (>300)	4.76

Source: own study.

Table 9. Sample classifications for water quality based on water quality index (*WQI*) and groundwater pollution index (*GPI*) values

Sample	*WQI*	Interpretation	*GPI*	Interpretation
S1	42.14	excellent	0.514	negligible pollution
S3	38.30	excellent	0.528	negligible pollution
S4	47.54	excellent	0.527	negligible pollution
S5	33.66	excellent	0.446	negligible pollution
F1	35.37	excellent	0.466	negligible pollution
F2	49.24	excellent	0.571	negligible pollution
F3	101.44	permissible	0.727	negligible pollution
F4	84.32	good	0.773	negligible pollution
F5	264.57	doubtful	1.664	moderate pollution
F6	88.44	good	0.851	negligible pollution
F7	151.32	permissible	1.335	slight pollution
P1	57.58	good	0.604	negligible pollution
P2	389.13	unsuitable	2.756	very high pollution
P3	135.82	permissible	1.204	slight pollution
P4	54.95	good	0.602	insignificant pollution
P5	57.39	good	0.644	negligible pollution
P6	68.48	good	0.667	negligible pollution
F8	46.64	excellent	0.541	negligible pollution
F9	150.26	permissible	1.244	slight pollution
F10	37.44	excellent	0.557	negligible pollution
F11	39.28	excellent	0.508	negligible pollution

Source: own study.

CONCLUSIONS

Water quality assessment is a vital process for determining suitability for specific uses and implementing preventive measures against contamination-related degradation. In this study, the water quality index (*WQI*) and groundwater pollution index (*GPI*) were used together to complement each other and obtain more accurate and realistic results for evaluating groundwater conditions in the Guorriguer Plain. Results show that most of the aquifer system remains unpolluted, while moderate contamination was found at several sampling points along the central axis of the area. Contaminated samples tended to cluster in topographically low areas underlain by Quaternary evaporite deposits such as halite and gypsum. High salinity in these zones is linked to increased mineral dissolution caused by hydrogeochemical interactions and semi-arid climate conditions. These factors are also influenced by anthropogenic activities, including the use of fertilisers, evaporation of irrigation water, leakage of untreated sewage into the aquifer, and the proximity of the water table to the surface in certain regions, which promotes water evaporation and salt accumulation. These findings provide a scientific basis for policymakers to develop targeted water resource management strategies.

These strategies should include enhanced periodic monitoring of evaporite-affected zones to prevent worsening salinisation, especially under projected climate change scenarios; restrictions on intensive human activities in vulnerable topographic areas showing contamination indicators; and the adoption of sustainable management techniques such as water harvesting or artificial recharge to compensate for natural recharge deficits.

In conclusion, this study emphasises the need for an integrated approach that combines continuous monitoring, hydrogeochemical analysis, and spatial planning to ensure the long-term preservation of groundwater quality. It underscores the importance of adapting management strategies to the unique geological and climatic features of semi-arid regions.

CONFLICT OF INTERESTS

All authors declare that they have no conflict of interests.

REFERENCES

Adimalla, N. (2019) "Controlling factors and mechanism of groundwater quality variation in semiarid region of South India: an approach of water quality index (WQI) and health risk assessment (HRA)," *Environmental Geochemistry and Health*, 42(6), pp. 1725–1752. Available at: https://doi.org/10.1007/s10653-019-00374-8.

Adimalla, N. and Taloor, A.K. (2020) "Hydrogeochemical investigation of groundwater quality in the hard rock terrain of South India using Geographic Information System (GIS) and groundwater quality index (GWQI) techniques," *Groundwater for Sustainable Development*, 10, 100288. Available at: https://doi.org/10.1016/j.gsd.2019.100288.

Ahamad, A. *et al.* (2018) "Assessment of groundwater quality with special emphasis on nitrate contamination in parts of Varanasi City, Uttar Pradesh, India," *Applied Water Science*, 8(4), 115. Available at: https://doi.org/10.1007/s13201-018-0759-x.

Bahrami Asl, F. *et al.* (2025) "Prioritization of sanitary landfill criteria using a modified delphi approach and development of a tool for efficient site selection," *Avicenna Journal of Environmenttal Health Engineering*, 12(1), pp. 29–39. Available at: https://doi.org/10.34172/ajehe.550.

Barakat, A. *et al.* (2021) "Assessment of spatial and seasonal groundwater quality variation in a semi-arid environment using GIS and multivariate statistical analysis: A case study from the Fez-Meknes basin (Morocco)," *Environmental Science and Pollution Research*, 28(15), pp. 18824–18841. Available at: https://doi.org/10.1007/s11356-020-10948-0.

Barki, D.N. and Singa, P. (2014) "Water quality assessment in terms of water quality index," *Global Journal of Biology, Agriculture & Health Sciences*, 3(3), pp. 69–71. Available at: https://www.longdom.org/articles/water-quality-assessment-in-terms-of-water-quality-index.pdf (Accessed: August 10, 2025).

Boateng, T.K, *et al.* (2020) "Groundwater quality assessment using statistical approach and water quality index in Ejisu-Juaben Municipality, Ghana," *Environmental Earth Sciences*, 79(4), 73. Available at: https://doi.org/10.1007/s12665-020-8814-y.

Djelel, B. (2014) *Étude du fonctionnement hydrodynamique d'un aquifère fracturé – Application à la région de Tébessa (NE Algérie) [Study of the hydrodynamic functioning of a fractured aquifer – Application to the Tébessa region (NE Algeria)*. MSc Thesis. Jijel, Algeria: Mohamed Seddik Benyahia University.

Guenouche, F.Z. *et al.* (2024) "Assessing water quality in North-East Algeria: A comprehensive study using water quality index (WQI) and PCA," *Water Practice & Technology* 19(4), pp. 1232–1248. Available at: https://doi.org/10.2166/wpt.2024.073.

Hireche, S. (2014) *Multi-scale analysis of fracturing in the Eocene carbonate reservoir of the Gourigueur syncline (Tébessa region, Northeastern Algeria)*. MSc Thesis. Jijel, Algeria: Mohamed Seddik Benyahia University.

Horton, R.K. (1965) "An index-number system for rating water quality," *Journal of Water Pollution Control Federation*, 37(3), pp. 300–306.

Islam, Md. S. (2023) "Water analysis," in *Hydrogeochemical evaluation and groundwater quality*. Cham: Springer, pp. 37–64. Available at: https://doi.org/10.1007/978-3-031-44304-6_3.

Jayasankar, P. *et al.* (2024) "Water quality index: Composite measure of quality of water," in P. Aguilar-Zárate *et al.* (eds.) *The food-energy-water triangle for sustainable development*. New York: Apple Academic Press, pp. 255–267. Available at: https://doi.org/10.1201/9781003561453-12.

Jia, X. *et al.* (2020) "Groundwater depletion and contamination: Spatial distribution of groundwater resources sustainability in China," *Science of the Total Environment*, 672, pp. 551–562. Available at: https://doi.org/10.1016/j.scitotenv.2019.03.457.

Karunanidhi, D. *et al.* (2021) "Revealing drinking water quality issues and possible health risks based on Water Quality Index (WQI) method in the South India," *Environmental Geochemistry and Health*, 43, pp. 931–948. Available at: https://doi.org/10.1007/s10653-020-00613-3.

Kotowski, T. and Kachnic, M. (2016) "The geochemical study of groundwaters from Cenozoic aquifers in the Gwda catchment (Western Pomerania, Poland)," *Environmental Earth Sciences*, 75, 192. Available at: https://doi.org/10.1007/s12665-015-4962-x.

Kotowski, T. and Satora, S. (2016) "Analysis of the spatial variability of the concentrations of Na^+ and K^+ ions in the groundwater sourced in Southern Poland," *Environment Protection Engineering*, 42(2), pp. 5–18. Available at: https://doi.org/10.5277/epe160201.

Li, H. *et al.* (2023) "Application of comprehensive water quality labeling index method in water quality evaluation of Xiangjiang River," Available at: https://doi.org/10.1109/iccbd-ai62252.2023.00033.

Li, P., He, X. and Guo, W. (2019) "Spatial groundwater quality and potential health risks due to nitrate ingestion through drinking water: A case study in Yan'an City on the Loess Plateau of northwest China," *Human and Ecological Risk Assessment*, 25(1–2), pp. 11–31. Available at: https://doi.org/10.1080/10807039.2018.1553612.

Luo, H. *et al.* (2024) "Integrating water quality index (WQI) and multivariate statistics for regional surface water quality evaluation: Key parameter identification and human health risk assessment," *Water*, 16(23), 3412. Available at: https://doi.org/10.3390/w16233412.

Madhav, S. *et al.* (2018) "Geochemical assessment of groundwater quality for its suitability for drinking and irrigation purpose in rural areas of Sant Ravidas Nagar (Bhadohi), Uttar Pradesh," *Geology, Ecology, and Landscapes*, 2(2), pp. 127–136. Available at: https://doi.org/10.1080/24749508.2018.1452485.

Moeinzadeh, H., Yong, K.-T. and Withana, A. (2024) "A critical analysis of parameter choices in water quality assessment," *Water Research*, 258, 121777. Available at: https://doi.org/10.1016/j.watres.2024.121777.

Mukate, S. *et al.* (2019) "Development of new integrated water quality index (IWQI) model to evaluate the drinking suitability of water," *Ecological Indicators*, 101, pp. 348–354. Available at: https://doi.org/10.1016/j.ecolind.2019.01.034.

Pachiyappan, G., Cuddalore Thandapani, S. and Kumarasamy, V. (2025) "Geochemical insights and seasonal hydrodynamics of groundwater quality in Paramathi Velur Region, Namakkal, India," *Carpathian Journal of Earth and Environmental Sciences*, 20(1), pp. 47–56. Available at: https://doi.org/10.26471/cjees/2025/020/312.

Piper, A.M. (1944) "A graphic procedure in the geochemical interpretation of water-analyses," *Transactions, American Geophysical Union*, 25(6), pp. 914–928. Available at: https://doi.org/10.1029/TR025i006p00914.

Rao, N.S. *et al.* (2018) "Quality and degree of pollution of groundwater, using PIG from a rural part of Telangana State, India," *Applied Water Science*, 8, 227. Available at: https://doi.org/10.1007/s13201-018-0864-x.

Rice, E.W., Baird, R.B. and Eaton A.D. (2017) *Standard methods for the examination of water and wastewater*. 23rd ed. Washington, DC: APHA. Available at: https://yabesh.ir/wp-content/uploads/2018/02/Standard-Methods-23rd-Perv.pdf (Accessed: August 10, 2025).

Rodier, J., Legube, B. and Merlet, N. (2016) "Mémento chimique [Chemistry handbook]," in *L'analyse de l'eau [Water analysis]*. 10th edn. Paris: Dunod, pp. 1729–1737.

Sanad, H. *et al.* (2024) "Assessment of groundwater quality using the Pollution Index of Groundwater (PIG), Nitrate Pollution Index (NPI), Water Quality Index (WQI), Multivariate Statistical Analysis (MSA), and GIS approaches: A case study of the Mnasra Region, Gharb Plain, Morocco," *Water*, 16(9), 1263. Available at: https://doi.org/10.3390/w16091263.

Subba Rao, N. (2005) "Seasonal variation of groundwater quality in a part of Guntur District, Andhra Pradesh, India," *Environmental Geology*, 49(3), pp. 413–429. Available at: https://doi.org/10.1007/s00254-005-0089-9.

Subba Rao, N. (2012) "*PIG*: A numerical index for dissemination of groundwater contamination zones," *Hydrological Processes*, 26(22), pp. 3344–3350. Available at: https://doi.org/10.1002/hyp.8456.

Taloor, A.K., Thakur, P.K. and Jakariya, M. (2022) "Remote sensing and GIS applications in water science," *Groundwater for*

Sustainable Development, 19, 100817. Available at: https://doi.org/10.1016/j.gsd.2022.100817.

Verma, A., Yadav, B.K. and Singh, N.B. (2020) "Hydrochemical monitoring of groundwater quality for drinking and irrigation use in Rapti Basin," *SN Applied Sciences*, 2(3), 460. Available at: https://doi.org/10.1007/s42452-020-2267-5.

WHO (2011) *Guidelines for drinking-water quality*. 4th edn. Geneva, Switzerland: World Health Organization. Available at: https://iris.who.int/server/api/core/bitstreams/b437749a-43f7-472f-a6d9-42596e8ac0ae/content (Accessed: July 13, 2025).

Zahedi, S. (2017) "Modification of expected conflicts between drinking water quality index and irrigation water quality index in water quality ranking of shared extraction wells using multi criteria decision making techniques," *Ecological Indicators*, 83, pp. 368–379. Available at: https://doi.org/10.1016/j.ecolind.2017.08.017.